

Palbociclib has antitumour effects on *Pten*-deficient endometrial neoplasias

Maria Alba Dosil^{1,2}, Cristina Mirantes¹, Núria Eritja^{1,2}, Isidre Felip¹, Raúl Navaridas¹, Sònia Gatiús^{1,2}, Maria Santacana^{1,2}, Eva Colàs³, Cristian Moiola³, Joan Antoni Schoenenberger⁴, Mario Encinas⁵, Eloi Garí^{6†}, Xavier Matias-Guiu^{1,2†} and Xavier Dolcet^{1,2†*} 

¹ Oncologic Pathology Group, Departament de Ciències Mèdiques Bàsiques, Universitat de Lleida, Hospital Universitari Arnau de Vilanova, Institut de Recerca Biomèdica de Lleida, IRBLleida, Lleida, Spain

² Centro de Investigación Biomédica en Red de Oncología (CIBERONC), Madrid, Spain

³ Biomedical Research Group in Gynaecology, Vall Hebron Research Institute (VHIR), Universitat Autònoma de Barcelona, Barcelona, Spain

⁴ Department of Pharmacology, Hospital Universitari Arnau de Vilanova. Institut de Recerca Biomèdica de Lleida, IRBLleida, Lleida, Spain

⁵ Departament de Medicina Experimental, Universitat de Lleida, Institut de Recerca Biomèdica de Lleida, IRBLleida, Lleida, Spain

⁶ Cell Cycle Group, Departament de Ciències Mèdiques Bàsiques, Universitat de Lleida, Institut de Recerca Biomèdica de Lleida, IRBLleida, Lleida, Spain

*Correspondence to: X Dolcet, Departament de Ciències Mèdiques Bàsiques, Universitat de Lleida/IRBLleida, Ed Biomedicina I, Hospital Arnau de Vilanova, Av. Rovira Roure 80, 25198 Lleida, Spain. E-mail: dolcet@cmb.udl.cat

†Equal contributions.

Abstract

PTEN is one of the most frequently mutated genes in human cancers. The frequency of *PTEN* alterations is particularly high in endometrial carcinomas. Loss of *PTEN* leads to dysregulation of cell division, and promotes the accumulation of cell cycle complexes such as cyclin D1–CDK4/6, which is an important feature of the tumour phenotype. Cell cycle proteins have been presented as key targets in the treatment of the pathogenesis of cancer, and several CDK inhibitors have been developed as a strategy to generate new anticancer drugs. Palbociclib (PD-332991) specifically inhibits CDK4/6, and it has been approved for use in metastatic breast cancer in combination with letrozole. Here, we used a tamoxifen-inducible *Pten* knockout mouse model to assess the antitumour effects of cyclin D1 knockout and CDK4/6 inhibition by palbociclib on endometrial tumours. Interestingly, both cyclin D1 deficiency and palbociclib treatment triggered shrinkage of endometrial neoplasias. In addition, palbociclib treatment significantly increased the survival of *Pten*-deficient mice, and, as expected, had a general effect in reducing tumour cell proliferation. To further analyse the effects of palbociclib on endometrial carcinoma, we established subcutaneous tumours with human endometrial cancer cell lines and primary endometrial cancer xenografts, which allowed us to provide more translational and predictive data. To date, this is the first preclinical study evaluating the response to CDK4/6 inhibition in endometrial malignancies driven by *PTEN* deficiency, and it reveals an important role of cyclin D–CDK4/6 activity in their development. Copyright © 2017 Pathological Society of Great Britain and Ireland. Published by John Wiley & Sons, Ltd.

Keywords: *PTEN*; endometrial carcinoma; cyclin D1; CDK4/6; palbociclib

Received 14 September 2016; Revised 8 February 2017; Accepted 9 March 2017

No conflicts of interest were declared.

Introduction

Activation of phosphatidylinositol 3-kinase (PI3K)–protein kinase B promotes cell survival and proliferation. The most important negative regulator of this pathway is phosphatase and tensin homologue deleted on chromosome 10 (*PTEN*), which antagonizes PI3K activity by dephosphorylating phosphatidylinositol (3,4,5)-trisphosphate to phosphatidylinositol (4,5)-bisphosphate [1,2].

PTEN is one of the most frequently mutated genes in human cancers [3]. The frequency of *PTEN* alterations is particularly high in endometrial carcinomas

(ECs), which are the most common tumours of the female genital tract [4]. Nearly 70% of ECs show *PTEN* alterations [5].

The role of *PTEN* in carcinogenesis has been validated by the use of different knockout (KO) mouse models [6–8]. Recently, our group generated a tamoxifen-inducible *Pten* KO mouse model. Loss of *Pten* leads to extremely rapid and efficient development of endometrial hyperplasias and *in situ* carcinomas, prostate neoplasias, and thyroid hyperplasias [9].

It is well known that absence of *PTEN* triggers abnormal cell division and alters the expression of cell

cycle regulators such as cyclin D1 (CycD1) [9]. The cyclin D (CycD)–CDK4/6 signalling axis is important for cell division and tumour growth [10,11]. The D-type cyclin family comprises three different proteins (D1, D2, and D3), and their expression is induced upon cell exposure to mitogens. Therefore, D-type cyclins link the cell environment to the machinery that drives cell cycle progression [12,13]. Overexpression of the D-type cyclins and/or CDK4/6 proteins is commonly seen in a number of human tumours. CycD1 is overexpressed in numerous neoplasms of the prostate and endometrium [10,14–16]. Among breast cancers, overexpression is seen in 50% of cases [17].

CDK inhibition has been presented as a strategy to generate new anticancer drugs. The effectiveness of CDK4 and CDK6 inhibition in cancer is being assessed with highly selective inhibitors, such as palbociclib [10,18,19], which specifically inhibits CDK4/6, but not the other CDKs [20].

Here, we first studied *Pten*-driven tumorigenesis in the context of CycD1 deficiency. Next, we used a tamoxifen-inducible *Pten* KO mouse model and different approaches with human EC cell lines to assess the antitumour effects of palbociclib. Finally, we performed xenografting of primary EC to provide more translational research data. Our results demonstrate that palbociclib treatment triggers shrinkage of endometrial lesions and reduces tumour cell proliferation. To date, this is the first preclinical study evaluating the response to palbociclib in endometrial malignancies driven by *Pten* deficiency.

Materials and methods

Cell lines and culture conditions

EC cell lines were grown in two dimensions and in three-dimensional (3D) cultures as described previously [21,22].

Cell viability and cell cycle distribution analysis

Cell viability and cell cycle distribution were evaluated as described previously [21,23].

Isolation of endometrial epithelial cells and establishment of 3D cultures

Isolation of mouse endometrial epithelial cells and establishment of 3D cultures were performed as described previously [24]. When required, *Pten* deletion in endometrial cells isolated from Cre:ER^{T+/-} PTEN^{ff} mice was induced by adding tamoxifen (0.5 µg/ml) to the culture medium.

Bromodeoxyuridine (BrdU) incorporation

The protocol followed was that described previously [24].

Confocal imaging and evaluation of spheroid diameter

Images of endometrial epithelial spheroids were captured and digitized as described previously [25]. The diameter of epithelial glands was assessed by the use of image analysis software (ImageJ version 1.46r; NIH, Bethesda, MD, USA).

RNA extraction, reverse transcription (RT) polymerase chain reaction (PCR), and RT quantitative PCR (qPCR)

Total RNA was extracted according to the manufacturer's instructions (RNeasy Total RNA kit; Qiagen, Valencia, CA, USA). RNA was reverse transcribed to cDNA by use of a High Capacity cDNA Archive Kit (Applied Biosystems, Foster City, CA, USA). The cDNA product was used as a template for subsequent PCR.

Relative levels of mRNA were calculated with the $2^{-\Delta\Delta Ct}$ method, and Ct values were normalized to transcripts of the reference gene β -glucuronidase (*GUSB*). Taqman technology from Applied Biosystems was used for real-time qPCR analyses. The probes used are detailed in supplementary material, Table S1.

Animals

Mice were maintained as described previously [23]. The *in vivo* studies complied with Law 5/1995 and Act 214/1997 of the Autonomous Community (Generalitat de Catalunya) and EU Directive EEC 63/2010, and were approved by the Ethics Committee on Animal Experiments of the University of Lleida and the Ethics Commission in Animal Experimentation of the Generalitat de Catalunya.

Cre:ER^{T+/-} PTEN^{ff} mice were generated as described previously [9]. CycD1 KO mice were obtained from the Jackson Laboratory (Bar Harbor, ME, USA). Cre:ER^{T+/-} PTEN^{ff} CycD1^{-/-} mice were bred by crossing Cre:ER^{T+/-} PTEN^{ff} and CycD1^{-/-} mice (supplementary material, Figure S1A).

Immunodeficient SCID mice were maintained in specific pathogen-free conditions.

Tamoxifen

Tamoxifen was dissolved and administered as described previously [9].

Palbociclib

Palbociclib was obtained from (Pfizer, New York, NY, USA), and the powder was stored at room temperature, protected from light.

For *in vitro* experiments, a 2.5 mM stock solution of palbociclib was prepared in dimethyl sulphoxide and stored as single-use aliquots at -80°C .

For *in vivo* experiments, palbociclib was dissolved in sodium L-lactate (Sigma-Aldrich, St Louis, MO, USA)

buffer (50 mM, pH 4.0). Cre:ER^{T+/-} PTEN^{fl/fl} mice were given a single daily dose of 100 mg/kg palbociclib by oral gavage, starting 2 weeks after tamoxifen injection. For acute palbociclib treatment, Cre:ER^{T+/-} PTEN^{fl/fl} mice were treated for three consecutive days with 75, 100 or 150 mg/kg inhibitor. For survival experiments, mice received five doses weekly until they were killed. In each experiment, control mice were given vehicle according to the same schemes.

Subcutaneous xenografts and treatment

Subcutaneous HEC-1A cell-derived or MFE-296 cell-derived tumours were developed, maintained and measured as previously described [21]. When tumours reached 100 mm³, mice were treated by oral gavage with vehicle or 150 mg/kg palbociclib for 15 days.

Patient-derived tumour xenograft (PDX) establishment and treatment

All animal procedures were performed according to protocols approved by the Animal Experimentation Ethics Committee of Vall Hebron University Hospital.

A PDX, PDX741, was generated by the use of fresh primary tumour tissue from an endometrioid endometrial cancer patient by subcutaneous implantation in the flanks of mice. For evaluation of drug efficacy, small pieces of PDXs were surgically transplanted subcutaneously into 6-week-old female Swiss nude mice, and allowed to establish. When the tumours reached 200 mm³, mice were randomized into groups of four or five, and treated with vehicle or palbociclib (150 mg/kg). Mice were treated daily by oral gavage for 10 days. Tumours were measured twice weekly with a vernier caliper, and volumes were calculated as (length × width²)/2 = mm³.

Histopathology and immunohistochemistry

Histopathological and immunohistochemical studies were performed as described previously [23]. The antibodies used are detailed in supplementary material, Table S2.

Immunohistochemical results were graded by considering the intensity of the staining. A histological score was obtained by using an automated imaging system, the ACIS III Instrument (DAKO, Denmark). An intensity score was obtained from four different areas of each sample.

Proliferation analysis

Proliferation was calculated by the use of Ki67 and CycD1 immunohistochemistry as described previously [9].

Western blotting

Western blotting was performed as described previously [23], with the antibodies detailed in supplementary material, Table S2.

Statistical analysis

All experiments were performed at least three times. Statistical analyses were performed with GraphPad Prism 6.0 software. Values are presented as means ± standard errors of the mean (SEMs). Data were compared by the use of Student's *t*-test, one-way ANOVA, or two-way ANOVA, with *p* < 0.05 considered to be significant. The chi-square test was used to compare the incidence of histopathological lesions between groups. The Mantel–Cox test, followed by the Gehan–Breslow–Wilcoxon test, was used to compare survival of mice between groups.

Results

PTEN deletion enhances CycD1 expression

Previous studies have demonstrated that PTEN influences CycD1 expression, but the reported results are still controversial [26–28]. To address this issue, we used tamoxifen-inducible *Pten* KO mice [9], which rapidly develop endometrial intraepithelial neoplasias (EINs), thyroid hyperplasias and prostatic intraepithelial neoplasias between 6 and 8 weeks after tamoxifen-induced *Pten* deletion (supplementary material, Figure S2A–C).

On immunohistochemical analysis, we observed an increase in CycD1 expression after PTEN loss in the endometrium, thyroid and prostate (supplementary material, Figure S2A–C), and this was concomitant with increased Ki67 expression (supplementary material, Figure S2G). Moreover, CycD1 expression was increased in lysates from endometrial epithelial 3D cultures, and thyroid or prostate tissues (supplementary material, Figure S2D–F). Collectively, these results indicate that PTEN loss increases CycD1 expression.

Effects of CycD1 deficiency in *Pten*-driven neoplasias

Having demonstrated that *Pten* deficiency correlated with an increase in CycD1 expression, we questioned whether such an increase was required to drive *Pten* loss-induced tumourigenesis. We generated Cre:ER^{T+/-} PTEN^{fl/fl} CycD1^{-/-} mice to achieve simultaneous loss of *Pten* and CycD1 (supplementary material, Figure S1A). The phenotype of mice lacking CycD1 compromised the viability of Cre:ER^{T+/-} PTEN^{fl/fl} CycD1^{-/-} mice, which limited the number of mice used in the study.

The experimental workflow is shown in Figure 1A and supplementary material, Figures S3A and S4A. Interestingly, CycD1 absence led to a reduction in the incidence and progression of endometrial lesions (Figure 1B). The majority of histological changes found in the endometrium of Cre:ER^{T+/-} PTEN^{fl/fl} CycD1^{-/-} mice were classed as hyperplasias, and only 17% of the mice progressed to EIN, whereas the EIN incidence in the wild-type (WT) counterparts was nearly 53%. Macroscopic analysis revealed no reduction in the size

of the thyroid (supplementary material, Figure S3B) or prostate (supplementary material, Figure S4B) of Cre:ER^{T+/-} PTEN^{fl/fl} CycD1^{-/-} mice. Furthermore, histological examination revealed that CycD1 deficiency did not impair PTEN tumorigenesis either in the thyroid or in the prostate (supplementary material, Figures S3C and S4C).

By using Ki67 immunohistochemistry, we found that the endometrium, thyroid and prostate from mice of both genotypes showed the same proliferation rate (Figure 1C, and supplementary material, Figures S3D and S4D, respectively). Finally, we analysed the expression of several components of the cell cycle in all three tissues from Cre:ER^{T+/-} PTEN^{fl/fl} CycD1^{+/+} and Cre:ER^{T+/-} PTEN^{fl/fl} CycD1^{-/-} mice. As shown in Figure 1D and supplementary material, Figures S3E and S4E, absence of CycD1 did not modify the expression of any of the elements analysed.

Finally, we also analysed the phosphorylation status of Rb as a biomarker of cyclin D–CDK4/6 activity. Immunohistochemistry for p-Rb (Ser780), which is specifically phosphorylated by CDK4/6, revealed no blockade of the cyclin D–CDK4/6 axis in the context of CycD1 absence (Figure 1E; supplementary material, Figures S3F and S4F). These results strongly support the hypothesis that proliferation of *Pten*-deficient malignancies is not dependent on CycD1.

CDK4/6 inhibition triggers an antiproliferative effect in mouse *Pten*-deficient endometrial cells *in vitro*

In an attempt to understand the molecular basis of the CycD1-independent proliferation and cell cycle progression in *Pten*-deficient tumours, we hypothesized that compensatory expression of other cyclins may override the loss of CycD1. We determined, by RT-qPCR, the levels of all three D-type cyclin transcripts from *Pten*-proficient and *Pten*-deficient epithelial endometrial 3D cultures. As shown in supplementary material, Figure S5A, *Pten* ablation induced upregulation not only of CycD1 mRNA expression, but also of cyclin D2 (CycD2) and cyclin D3 (CycD3).

It seemed that loss of PTEN enhanced the expression of all of the D-type cyclins, making the absence of a single CycD insufficient to impede the CycD–CDK4/6 axis. To override the redundancy of D-type cyclins, we decided to evaluate the impact of CycD–CDK4/6 signaling axis inhibition on cell proliferation. For this purpose, we established endometrial 3D cultures from Cre:ER^{T+/-} PTEN^{fl/fl} mice treated (*Pten* KO) or not treated (*Pten* WT) with tamoxifen to induce *Pten* excision. The 3D cultures were exposed to palbociclib for 48 h. Palbociclib treatment resulted in significant decreases in glandular size (supplementary material, Figure S5B) and the number of BrdU-incorporating cells (supplementary material, Figure S5C). All of the above results demonstrate that CDK4/6 inhibition by palbociclib induces a decrease in endometrial cell proliferation *in vitro*.

Palbociclib treatment reduces *Pten*-induced EC *in vivo*

Next, we sought to investigate whether the inhibitor was equally effective *in vivo* in our tamoxifen-inducible *Pten* KO mouse model. The treatment scheme is shown in Figure 2A. Histopathological evaluation revealed that palbociclib-treated mice had endometrial lesions to a significantly lower extent than untreated mice. Vehicle-treated mice showed EIN (67%) and severe hyperplasia (33%), whereas most mice receiving palbociclib showed hyperplasia (40%) and severe hyperplasia (40%). Moreover, only 10% of the lesions progressed to EIN, and another 10% retained normal histology (Figure 2B). In addition, uteri from Cre:ER^{T+/-} PTEN^{fl/fl} mice treated with the inhibitor showed a substantial reduction in expression of the Ki67 proliferation marker in comparison with untreated mice (Figure 2C).

In other tissues, macroscopic analysis revealed dramatic reductions in thyroid and prostate size and weight (supplementary material, Figures S6B and S7B) from Cre:ER^{T+/-} PTEN^{fl/fl} mice treated with palbociclib, following the treatment schemes shown in supplementary material, Figures S6A and S7A. Moreover, Ki67 expression was also reduced in both tissues treated with the inhibitor (supplementary material, Figures S6D and S7D), indicating that palbociclib is effective at decreasing tumour cell proliferation in both the thyroid and the prostate. Surprisingly, histopathological analysis revealed that the incidence of neither thyroid hyperplasia nor prostate neoplasia was reduced by palbociclib (supplementary material, Figures S6C and S7C).

Endometrial neoplasia response to palbociclib correlates with Rb phosphorylation on Ser780 *in vivo*

To investigate the underlying molecular mechanism explaining the antitumour effect of palbociclib *in vivo* on the endometrium, we used immunohistochemistry to analyse the levels of p-Rb (Ser780) in the tissues after short-term or long-term treatment with the inhibitor.

The experimental workflow diagram for short-term treatment is shown in Figure 3A. Palbociclib treatment led to a potent reduction in the level of p-Rb (Ser780) in the endometrium, regardless of the dose tested (Figure 3B; supplementary material, Figure S8A). Surprisingly, the reduction in p-Rb (Ser780) level was not observed in the endometrium after 21 days of treatment (Figure 3C; supplementary material, Figure S8B). In our hands, palbociclib was not effective at reducing Rb phosphorylation in either the thyroid or the prostate (Figure 3B, C; supplementary material, Figure S8C, D).

It has been suggested that, in the absence of CycD–CDK4/6 activity, the phosphorylation of Rb could be carried out by cyclin E (CycE)–CDK2 in a scenario with low activity of CDK inhibitors such as p27 [12,31,32]. After long-term treatment with palbociclib in the endometrium, our results pointed to two different situations. On the one hand, some mice

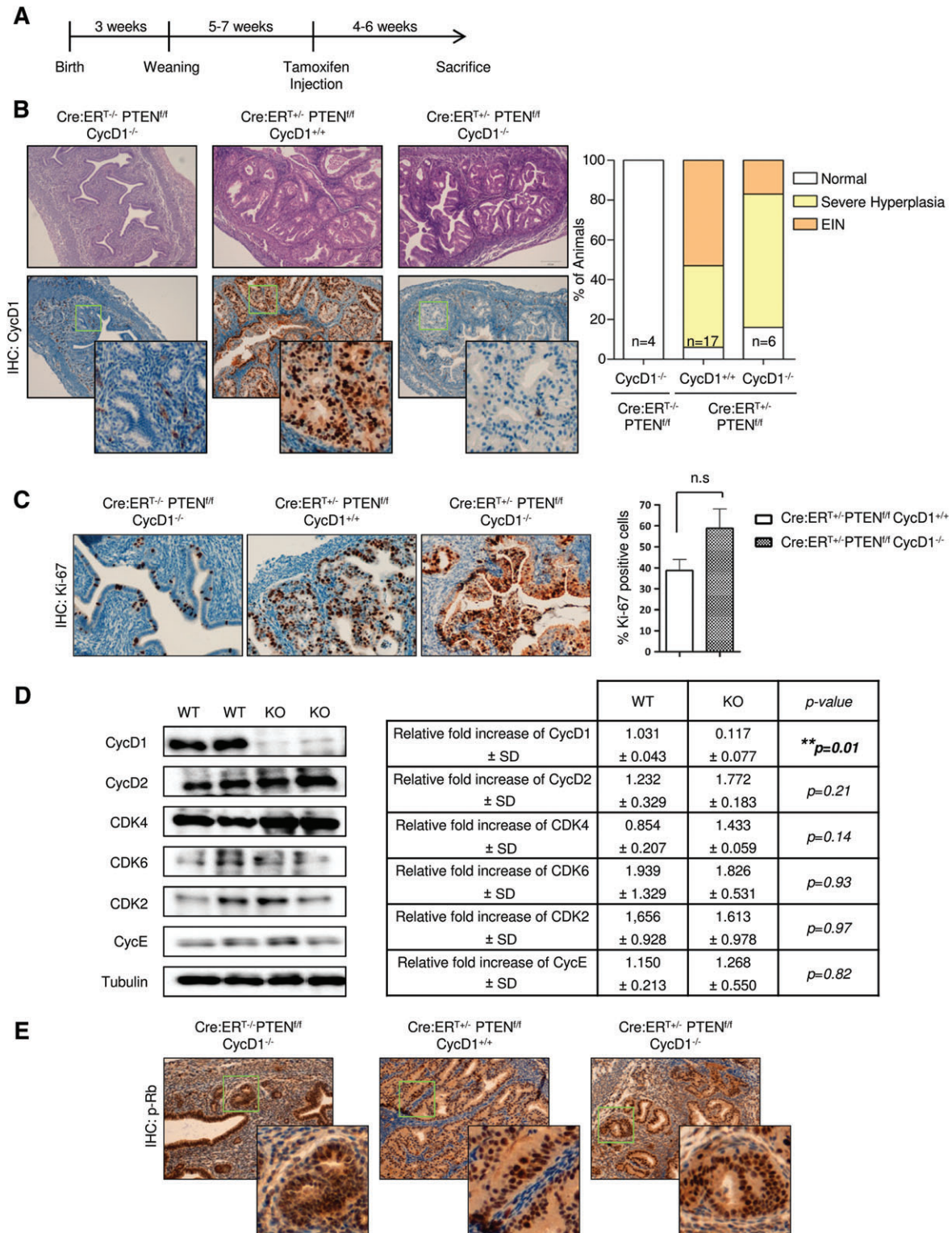


Figure 1. CycD1 deficiency results in a slight reduction in endometrial lesions. (A) Schematic diagram showing the experimental workflow. In short, mice were weaned 3 weeks after birth. At 8–10 weeks of age, mice were injected with a single dose of tamoxifen to achieve *Pten* ablation. Mice were killed 4–6 weeks later. (B) Representative images showing haematoxylin and eosin staining (top panels) and immunostaining for CycD1 (bottom panels) on uteri collected from Cre:ER^{T-/-} PTEN^{fl/fl} CycD1^{-/-}, Cre:ER^{T+/-} PTEN^{fl/fl} CycD1^{+/+} and Cre:ER^{T+/-} PTEN^{fl/fl} CycD1^{-/-} mice (×10), and evaluation of endometrial histology. Chi-square analysis showed no significant differences. (C) Representative images and quantification of Ki67 immunostaining. Data are from five mice for each genotype, and values are mean ± SEM. No significant differences were observed on *t*-test analysis. (D) Evaluation of CycD1, CycD2, CDK4, CDK6, CDK2 and CycE expression by western blotting in uteri collected from Cre:ER^{T+/-} PTEN^{fl/fl} CycD1^{+/+} (WT) and Cre:ER^{T+/-} PTEN^{fl/fl} CycD1^{-/-} (KO) mice. A representative image of three biological replicates is shown for each genotype. Tubulin served as loading control. Immunoreactive bands were quantified by densitometry analysis with ImageJ software. Relative level values are expressed with tubulin as a reference. ***p* < 0.01, *t*-test. (E) Representative images of p-Rb (Ser780) immunostaining. IHC, immunohistochemistry; SD, standard deviation.

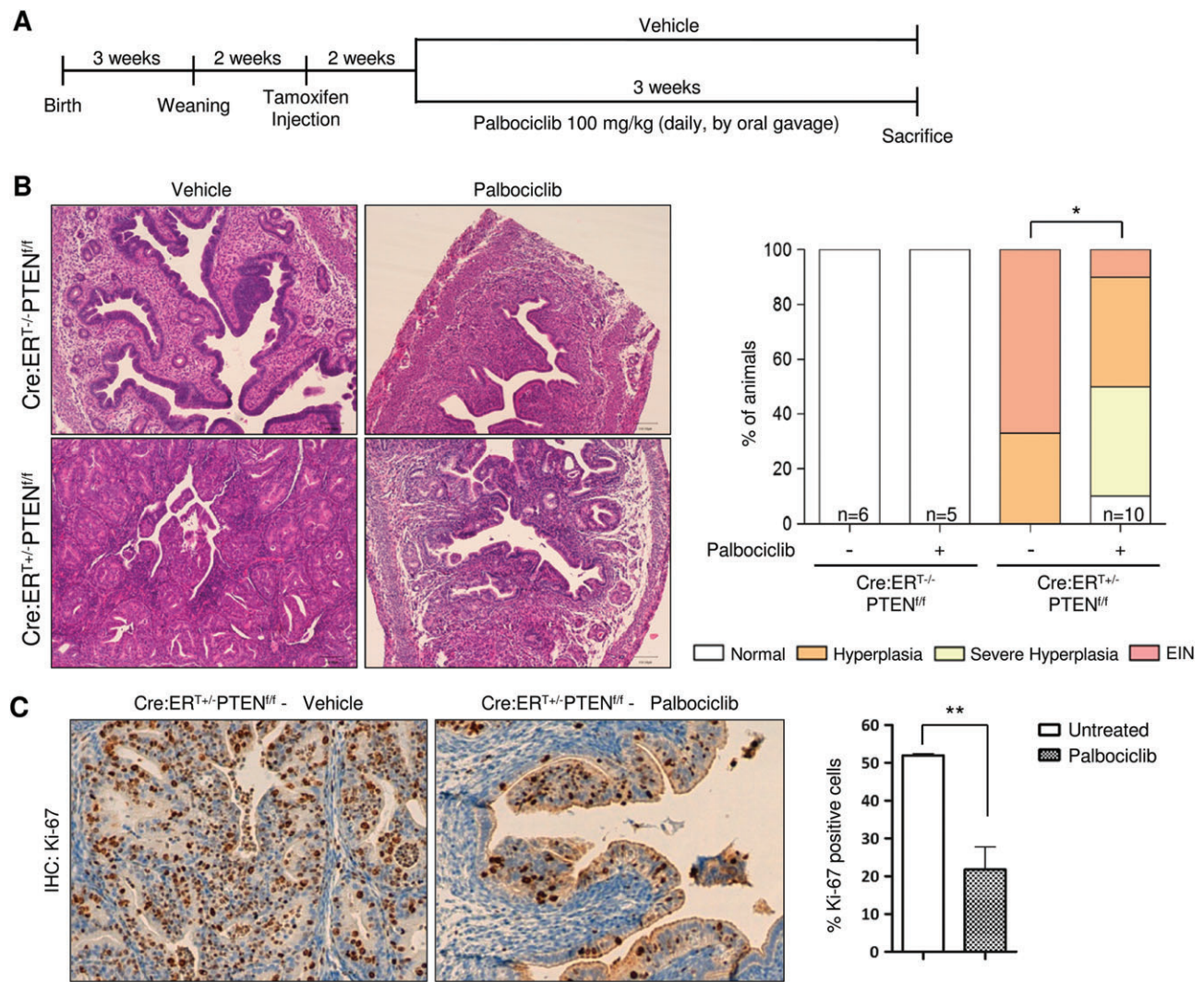


Figure 2. Palbociclib treatment reduces ECs in *Pten*-deficient mice. (A) Schematic representation of the protocol used for palbociclib administration. In brief, mice were given a single daily dose of 100 mg/kg of the drug for 21 consecutive days, starting 2 weeks after *Pten* deletion. (B) Representative images of haematoxylin and eosin staining (×10) and evaluation of uterine lesions from untreated and palbociclib-treated mice. **p* < 0.05, chi-square test. (C) Representative images and quantification of Ki67 immunostaining performed on uteri dissected from mice treated or not treated with the drug. Data are from five mice for each genotype, and values are mean ± SEM. ***p* < 0.01, *t*-test. IHC, immunohistochemistry.

showed high levels of phosphorylated extracellular signal-related kinase (p-ERK), and this increase was concomitant with high levels of CycD1, CycE, p27, and p-Rb. On the other hand, mice with lower levels of p-ERK showed lower levels of CycD1, CycE, p27, and p-Rb. No significant changes in p-AKT, p-S6K and CDK2 levels were observed (supplementary material, Figure S8E). Even though the presence of palbociclib abrogates CycD–CDK4/6 activity, these findings led us to hypothesize that D-type cyclins present in the cells still bind to CDK inhibitors, allowing CycE–CDK2 complexes to phosphorylate Rb.

Palbociclib treatment slows down EC progression and increases overall survival of mice

The therapeutic benefits of palbociclib (administered for 21 days) on *Pten*-deficient ECs encouraged us to study

the effects of chronic exposure to the inhibitor. The treatment scheme is shown in Figure 4A. Chronic treatment with palbociclib resulted in significantly increased survival of mice. Cre:ER^{T+/-}PTEN^{fl/fl} treated females had a median survival of 47 days, whereas this value was reduced to 32 days for the untreated ones (Figure 4B).

In the endometrium, palbociclib induced a delay in the development of EIN after *Pten* loss. However, palbociclib-treated females finally showed severe hyperplasia and EIN (Figure 4E). As shown in Figure 4C, D, macroscopic and histological analysis revealed no differences between *Pten*-deficient thyroids treated or not treated with the inhibitor. Collectively, these results suggest that palbociclib treatment slows down tumour progression, allowing longer survival. Nevertheless, it does not cause significant regression of endometrial and thyroid malignancies induced by *Pten* loss.

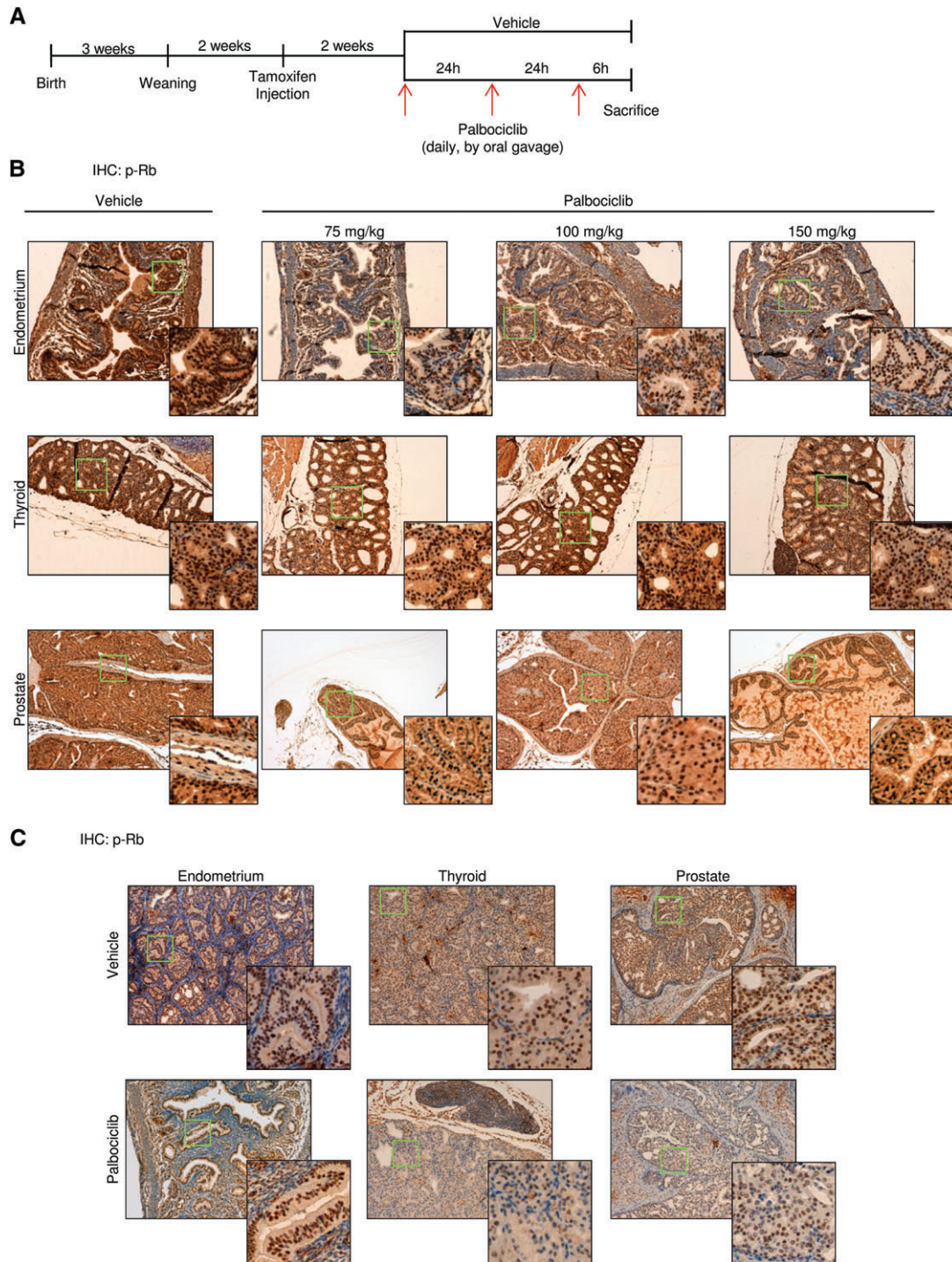


Figure 3. Tumour responses to palbociclib in the endometrium correlate with Rb phosphorylation on Ser780 *in vivo*. (A) Experimental workflow diagram showing the procedure used for acute palbociclib treatment. Briefly, mice were treated with 75, 100 or 150 mg/kg palbociclib for three consecutive days, starting 2 weeks after *Pten* deletion. (B) Representative images of p-Rb immunostaining performed on uteri (upper panel), thyroids (central panel) and prostates (bottom panel) dissected from mice after a short course of palbociclib. (C) Representative images of p-Rb immunostaining performed on uteri (left), thyroids (central panel) and prostates (right) dissected from mice after 21 days of treatment with palbociclib. IHC, immunohistochemistry.

Palbociclib induces an antiproliferative effect *in vitro* on human EC cell lines

It has been reported previously that palbociclib treatment reduces the proliferation of multiple human tumour cell lines [33]. Having demonstrated the drug's antitumour effect in *Pten*-deficient ECs in mice, we

aimed to determine its therapeutic potential in different human EC models. We first monitored the viability of two EC cell lines, HEC-1A and MFE-296, after palbociclib treatment by using an MTT cytotoxicity assay. Both cell lines exposed to different concentrations of palbociclib (2.5, 5 and 10 μM) for 48 h showed significantly decreased cell viability (supplementary

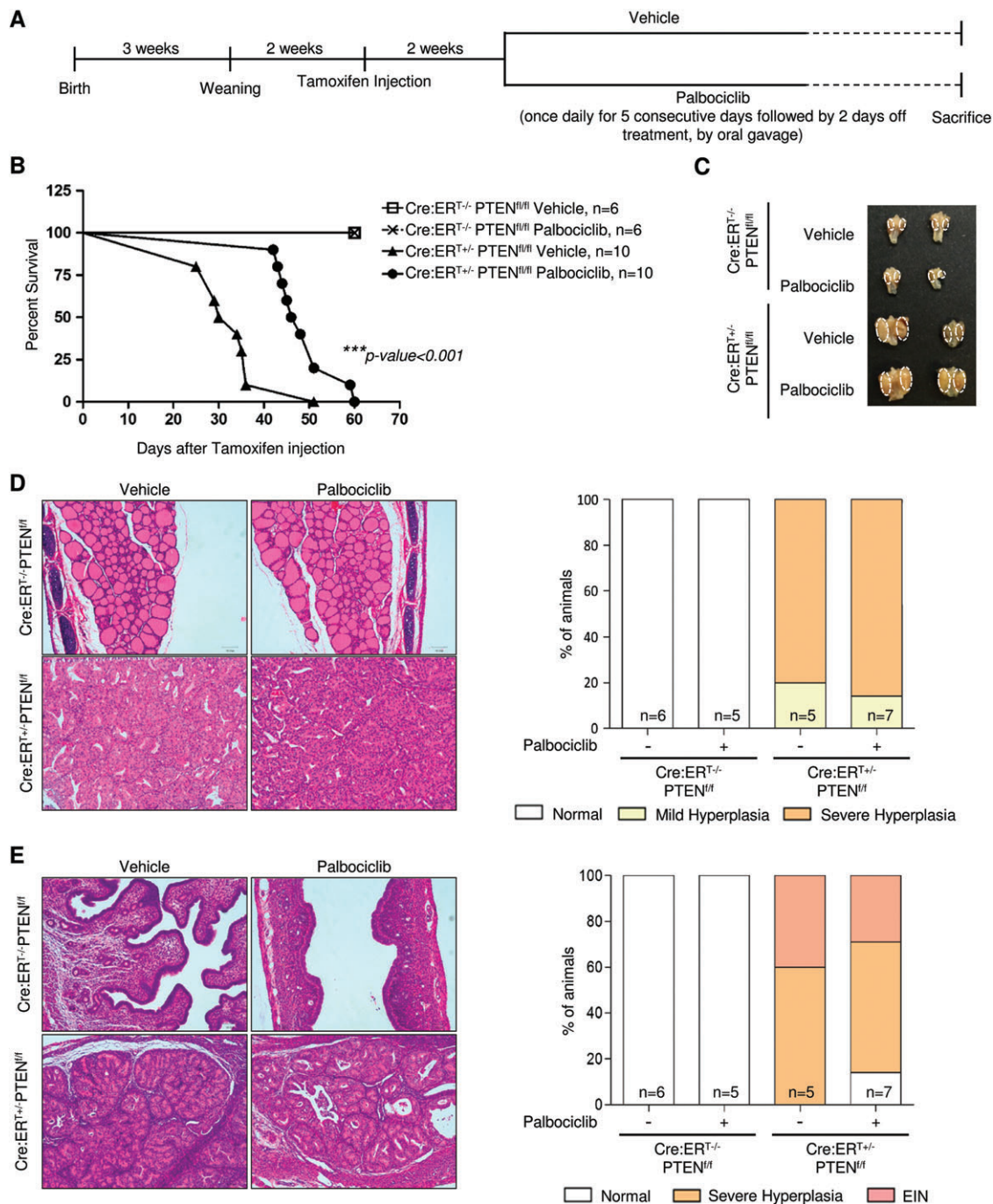


Figure 4. Effects of chronic palbociclib treatment in *Pten*-deficient ECs and thyroid hyperplasias. (A) Schematic representation of the protocol used for palbociclib administration. Briefly, mice were given a single daily dose of 100 mg/kg palbociclib for five consecutive days, and this was followed by 2 days off treatment until mice were killed, starting 2 weeks after *Pten* deletion. (B) Kaplan–Meier survival curve. ****p* < 0.001, Mantel–Cox test, followed by the Gehan–Breslow–Wilcoxon test. (C) Macroscopic images of thyroids from palbociclib-treated and untreated mice. (D) Representative images of haematoxylin and eosin (H&E) staining (×10) and evaluation of thyroid lesions. No significant differences were observed on chi-square analysis. (E) Representative images of H&E staining (×10) and evaluation of uterine lesions from palbociclib-treated and untreated mice. No significant differences were observed by chi-square analysis.

material, Figure S9A). We also observed that treatment of HEC-1A and MFE-296 cells with 5 and 10 μM palbociclib for 48 h resulted in G₁-phase arrest, preventing cells from entering S-phase (supplementary material, Figure S9B). Finally, as shown in supplementary material, Figure S9C, palbociclib also significantly reduced the glandular size of HEC-1A cells when they were grown in 3D cultures.

Palbociclib shows antitumour activity against human EC

Given that palbociclib showed antiproliferative effects on EC cell lines *in vitro*, we aimed to assess whether the inhibitor has antitumour activity *in vivo*. Mice with HEC-1A or MFE-296 subcutaneous tumours were treated daily with palbociclib at a dose of 150 mg/kg

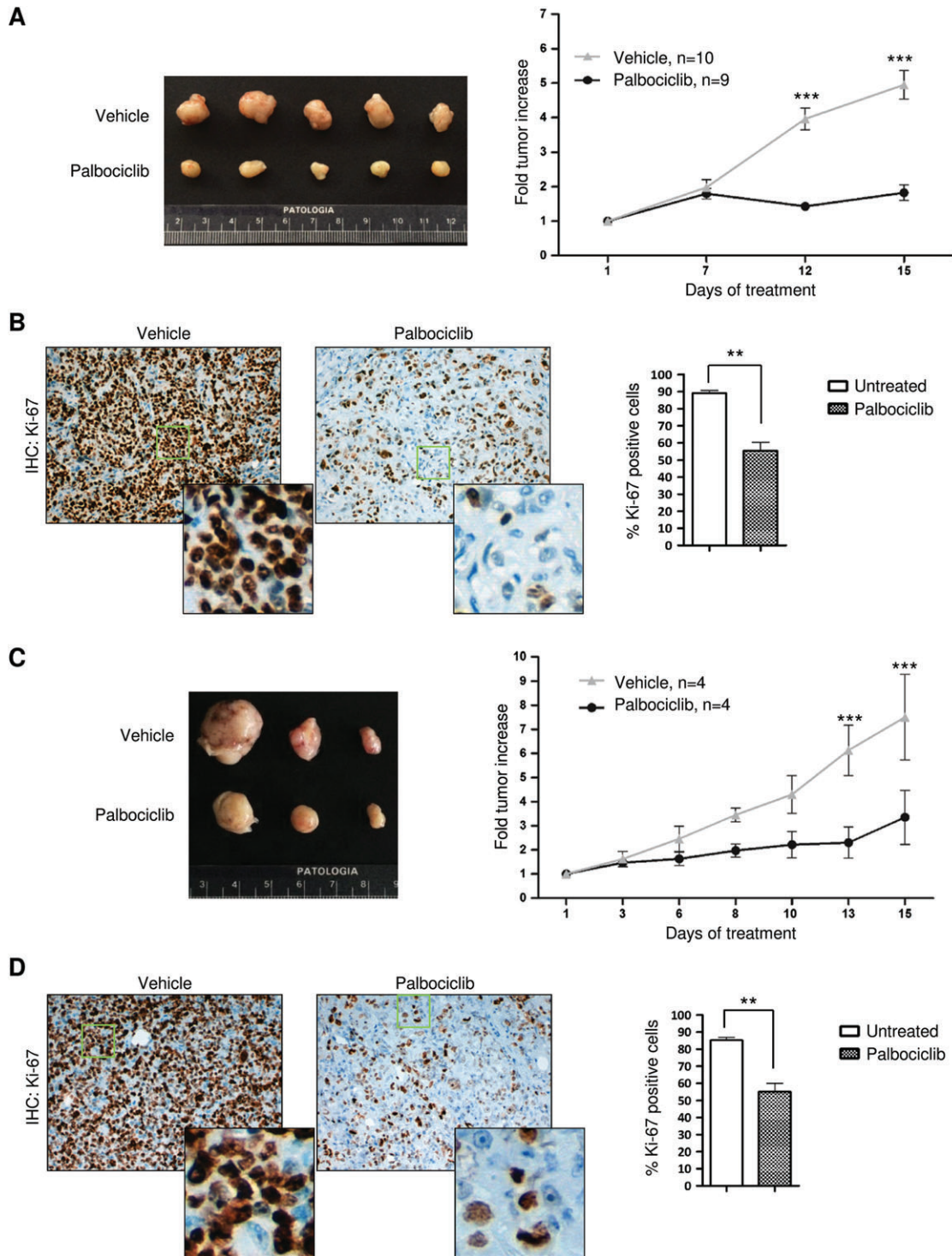


Figure 5. Palbociclib treatment reduces *in vivo* growth of EC cell line tumours. SCID mice bearing HEC-1A or MFE-296 subcutaneous tumours were treated daily by oral gavage with 150 mg/kg palbociclib for 15 days. (A, C) Comparison of representative vehicle and palbociclib-treated HEC-1A (A) or MFE-296 (C) xenograft tumours, and graphs of tumour growth over time. $***p < 0.001$, two-way ANOVA followed by the Bonferroni *post hoc* comparison test. (B, D) Representative images and quantification of Ki67 immunostaining performed on HEC-1A (B) or MFE-296 (D) subcutaneous tumours from mice treated or not treated with the drug. Data are from four mice for each group, and values are mean \pm SEM. $**p < 0.01$, *t*-test. IHC, immunohistochemistry.

for 15 days by oral gavage. Interestingly, palbociclib treatment led to a significant reduction in tumour growth (Figure 5A, C) with a concomitant decrease in Ki67 expression (Figure 5B, D) as compared with vehicle-treated mice. Taken together, these data indicate that palbociclib inhibits tumour growth of

subcutaneously injected HEC-1A and MFE-296 cell lines in SCID mice.

In order to circumvent the limitations of conventional preclinical models in terms of translational research, we also generated a PDX model by using a primary PTEN-deficient endometrioid EC

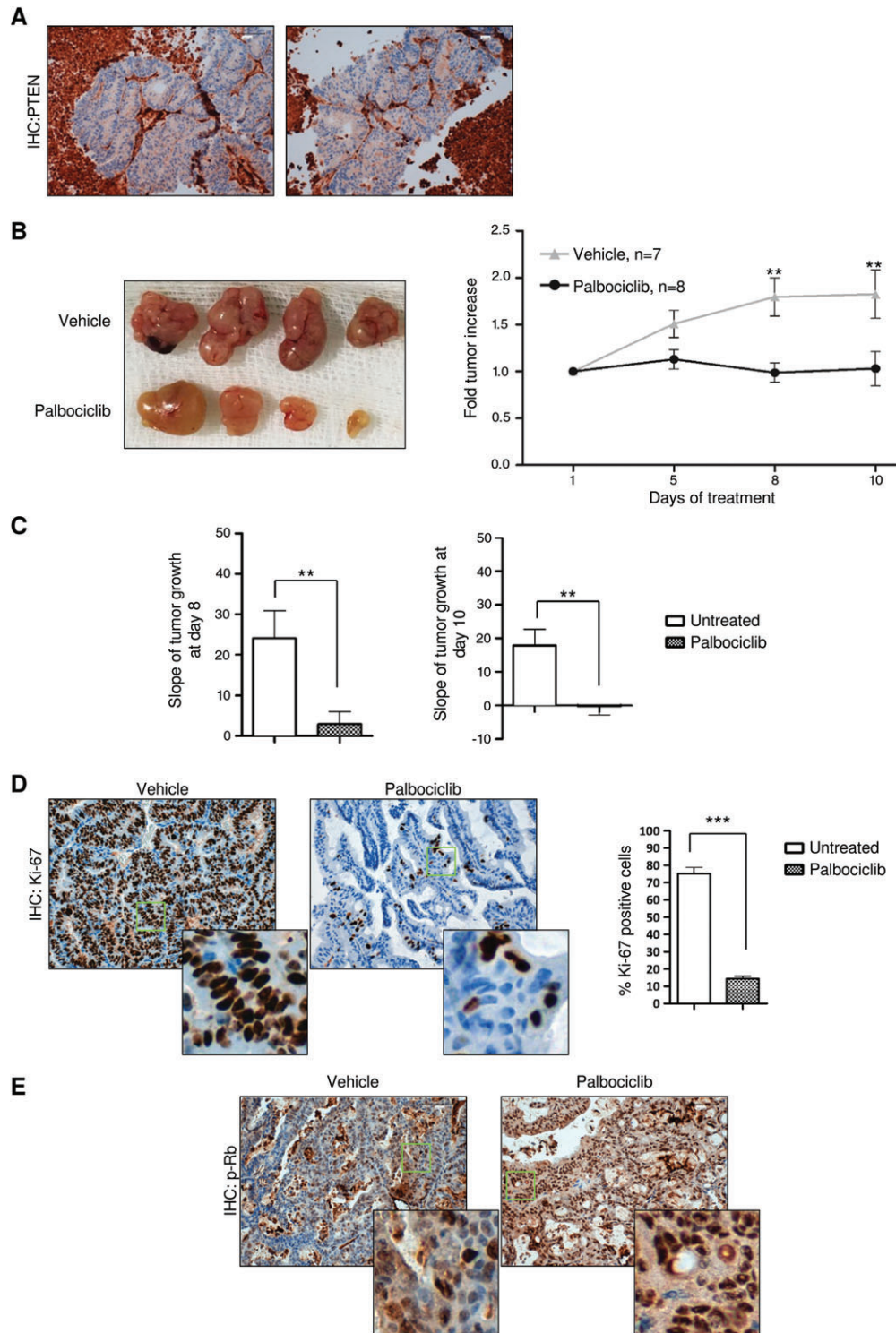


Figure 6. CDK4/6 inhibition by palbociclib in a PTEN-deficient PDX impairs endometrial carcinogenesis. (A) Representative images of PTEN immunostaining performed on patient-derived endometrioid EC. (B) Comparison of representative vehicle-treated and palbociclib-treated PDXs, and graph of tumour growth over time. $**p < 0.01$, two-way ANOVA, followed by the Bonferroni *post hoc* comparison test. (C) Slope of tumour growth at days 8 and 10 of treatment. $**p < 0.01$, *t*-test. (D) Representative images and quantification of Ki67 immunostaining performed on PDXs treated or not treated with the drug. Data are from $n = 3$ for each group, and values are mean \pm SEM. $***p < 0.001$, *t*-test. (E) Representative images of p-Rb immunostaining performed on PDXs treated or not treated with palbociclib. IHC, immunohistochemistry.

(Figure 6A). EC material was injected subcutaneously into female mice, and the effects of palbociclib were assessed for 10 days. As shown in Figure 6B, C, palbociclib decreased tumour growth in those mice treated with the drug. Furthermore, PDXs

treated with palbociclib showed marked reductions in Ki67 expression as compared with untreated ones (Figure 6D). Finally, no significant reductions in p-Rb levels were observed after palbociclib treatment (Figure 6E).

Discussion

In the present study, we investigated the role of the CycD–CDK4/6 axis in *Pten*-deficient ECs.

We observed that ECs induced by *Pten* loss show higher expression of CycD1 than normal tissue, consistent with previous evidence [34]. However, the direct effect of PTEN on CycD1 expression is controversial. For instance, it has been reported that the mutant PTEN-G129E form reduces CycD1 levels in a breast cancer model [28]. Some ECs have some mutations in this lipid-phosphatase domain (G129D/E/R/V). It will be interesting to determine the effects of these PTEN mutant forms on CycD1 levels. Nevertheless, our results are not comparable with those mentioned above, because we worked with a model of PTEN loss. We focused on *Pten*-deficient ECs, as they represent an important proportion of the total cases. Therefore, it seems that CycD1 participates somehow in *Pten*-driven endometrial malignancies, but the underlying mechanism has not been completely elucidated.

Here, we have evaluated the efficacy of palbociclib in ECs in *Pten*-deficient mice. Our results showed that palbociclib reduces tumour cell proliferation and disrupts the tumorigenic process in the endometrium. Interestingly, CycD1 deficiency alone decreases the extent of endometrial lesions.

It is noteworthy that our results suggest that thyroid and prostate *Pten*-deficient tumour maintenance is dependent on the CycD–CDK4/6 axis, because palbociclib decreases cell proliferation in both tissues. Consistent with this, Comstock *et al* have reported antiproliferative effects of palbociclib on prostate human tumour tissues *ex vivo* [35]. Surprisingly, neither prostate nor thyroid tumorigenesis was disrupted after palbociclib administration in our mouse model. However, a functional collaboration between p18 and PTEN in tumour suppression has been reported [36]. In this model, the activity of the CycD–CDK4/6 axis is increased during development and before the appearance of tumours. In contrast, in our model, palbociclib is given at the onset of malignancies. The distinct temporal interventions can lead to different response patterns. A question raised is why thyroid and prostate malignancies are dependent on CycD–CDK4/6 inhibition for tumour maintenance but not for tumorigenesis. This answer could lie in the proliferation-independent functions of the CycD–CDK4/6 axis [37].

Therapeutic intervention in the cell cycle has been proposed as an effective antitumour therapy [38,39]. Numerous clinical trials are ongoing to determine any therapeutic benefit of palbociclib, either alone or in combinatorial approaches [38–40]. PDXs offer an advanced preclinical model [41,42]. Here, we provide evidence that palbociclib has therapeutic potential in a model of primary PTEN-deficient EC. However, palbociclib has failed to induce tumour regression and cytotoxic effects. It is imperative to develop palbociclib combinations with some cytotoxic agents. Some *in vitro*

studies performed with breast cancer cell lines have reported antagonistic activity between palbociclib and some chemotherapeutics [43,44]. Nevertheless, with proper cell cycle synchronization, a synergistic killing effect has been achieved in multiple models [45–47]. It is worth noting that palbociclib is the first cell cycle inhibitor to demonstrate broad-ranging efficacy in many tumour types. Therefore, it seems reasonable to consider that palbociclib combinations potentially offer great promise [40].

Data from several groups have indicated that the status of p-Rb is critical for palbociclib activity [33,35,38–40], and that loss of Rb leads to drug resistance [38]. In our model, palbociclib treatment reduces p-Rb levels in the endometrium after acute treatment, but not in other tissues or with longer treatments. Restoration of p-Rb levels may explain why palbociclib fails to cause disease regression in the endometrium after long-term treatment. However, the role of Rb as a prognostic factor for palbociclib treatment is still unclear. Consistent with this, we have found that PDX samples, which showed reduced proliferation and tumour growth after palbociclib treatment, do not show decreased levels of p-Rb. Furthermore, it has been reported that some patients who do not show any benefit after palbociclib treatment have decreased p-Rb levels [38,44,48]. In these cases, the presence of intact Rb function does not predict CDK4/6 dependence.

During cell division, CycD–CDK4/6 sequesters CDK inhibitors such as p27, liberating CycE–CDK2 activity, which, in turn, results in the phosphorylation of Rb. Similar reasoning could be used to explain the presence of p-Rb during palbociclib treatment. However, after long-term treatment with palbociclib, we observed two possible scenarios. On the one hand, we observed low levels of CycD1, p27, and CycE. On the other hand, after ERK activation, we detected upregulation of the mentioned proteins, which correlated with an increase in p-Rb levels. We propose here that, although palbociclib inhibits CycD–CDK4/6 kinase activity, CycD1 still retains the ability to sequester p27 and release CycE. In this way, CycE expression may be enough for Rb to be phosphorylated when it is associated with CDK2 [12,31,32]. Moreover, it is known that ERK pathway activation is necessary and sufficient to induce CycD1 expression [49], so, in the second context, the huge amount of CycD1 may bypass palbociclib inhibition and also phosphorylate Rb. Furthermore, it would be interesting to determine the mechanism by which CycE is upregulated. We hypothesize that CycE may be responsible for Rb phosphorylation during palbociclib inhibition, as previously described [12]. Consistent with these findings, we have shown here that p-Rb levels are increased in those mice expressing more CycE.

In conclusion, we report the first preclinical study in which the therapeutic potential of palbociclib has been evaluated in endometrial malignancies driven by *Pten* deficiency. Our results highlight the clinical potential of palbociclib as an antitumour drug in the endometrium.

Acknowledgements

This work was supported by grants FIS PI13/00263, SAF2016-80157-R, PI13/01701, 2009SGR794, Grupos estables AECC (AECC2011), RETICS (RD12/0036/0013), Catalunya contra el càncer, Programa de intensificació de la investigació, Instituto Carlos III, and BFU 2013-42895-P. MAD holds a predoctoral fellowship from Ministerio de Educación. We thank Mónica Domingo, Lidia Parra, Maria Carrelé and Anais Panosa for their technical support.

Author contributions statement

The authors contributed in the following way: MAD, CM, EG, XD, XMG: conceived experiments; MAD, CM, RN, MS, EC, CMo: performed experiments; MAD, CM, NE, SG, JAS, ME, EG, XMG, XD: analysed data; MAD, EG, XD: wrote the paper; MAD, NE, IF: generated figures. All authors approved the submitted and published versions.

References

- Maehama T, Dixon JE. The tumor suppressor, PTEN/MMAC1, dephosphorylates the lipid second messenger, phosphatidylinositol 3,4,5-trisphosphate. *J Biol Chem* 1998; **273**: 13375–13378.
- Myers MP, Tonks NK. PTEN: sometimes taking it off can be better than putting it on. *Am J Hum Genet* 1997; **61**: 1234–1238.
- Hollander MC, Blumenthal GM, Dennis PA. PTEN loss in the continuum of common cancers, rare syndromes and mouse models. *Nat Rev Cancer* 2011; **11**: 289–301.
- Amant F, Moerman P, Neven P, et al. Endometrial cancer. *Lancet* 2005; **366**: 491–505.
- Kandoth C, Schultz N, Cherniack AD, et al. Integrated genomic characterization of endometrial carcinoma. *Nature* 2013; **497**: 67–73.
- Suzuki A, de la Pompa JL, Stambolic V, et al. High cancer susceptibility and embryonic lethality associated with mutation of the PTEN tumor suppressor gene in mice. *Curr Biol* 1998; **8**: 1169–1178.
- Di Cristofano A, Pesce B, Cordon-Cardo C, et al. Pten is essential for embryonic development and tumour suppression. *Nat Genet* 1998; **19**: 348–355.
- Podszypanina K, Ellenson LH, Nemes A, et al. Mutation of Pten/Mmac1 in mice causes neoplasia in multiple organ systems. *Proc Natl Acad Sci U S A* 1999; **96**: 1563–1568.
- Mirantes C, Eritja N, Dosil MA, et al. An inducible knockout mouse to model the cell-autonomous role of PTEN in initiating endometrial, prostate and thyroid neoplasias. *Dis Model Mech* 2013; **6**: 710–720.
- Casimiro MC, Velasco-Velázquez M, Aguirre-Alvarado C, et al. Overview of cyclins D1 function in cancer and the CDK inhibitor landscape: past and present. *Expert Opin Investig Drugs* 2014; **23**: 295–304.
- Pestell RG. New roles of cyclin D1. *Am J Pathol* 2013; **183**: 3–9.
- Barrière C, Santamaría D, Cerqueira A, et al. Mice thrive without Cdk4 and Cdk2. *Mol Oncol* 2007; **1**: 72–83.
- Malumbres M, Barbacid M. Cell cycle, CDKs and cancer: a changing paradigm. *Nat Rev Cancer* 2009; **9**: 153–166.
- Bartkova J, Lukas J, Strauss M, et al. Cyclin D1 oncoprotein aberrantly accumulates in malignancies of diverse histogenesis. *Oncogene* 1995; **10**: 775–778.
- Cheung TH, Yu MM, Lo KW, et al. Alteration of cyclin D1 and CDK4 gene in carcinoma of uterine cervix. *Cancer Lett* 2001; **166**: 199–206.
- Dickson C, Fantl V, Gillett C, et al. Amplification of chromosome band 11q13 and a role for cyclin D1 in human breast cancer. *Cancer Lett* 1995; **90**: 43–50.
- Santamaría D, Ortega S. Cyclins and CDKs in development and cancer: lessons from genetically modified mice. *Front Biosci* 2006; **11**: 1164–1188.
- Malumbres M, Barbacid M. Cell cycle kinases in cancer. *Curr Opin Genet Dev* 2007; **17**: 60–65.
- Malumbres M, Pevarello P, Barbacid M, et al. CDK inhibitors in cancer therapy: what is next? *Trends Pharmacol Sci* 2008; **29**: 16–21.
- Gohil K. Pharmaceutical approval update. *Pharmacol Ther* 2015; **40**: 726–774.
- Eritja N, Domingo M, Dosil MA, et al. Combinatorial therapy using dovitinib and ICI182.780 (fulvestrant) blocks tumoral activity of endometrial cancer cells. *Mol Cancer Ther* 2014; **13**: 776–787.
- Eritja N, Chen BJ, Rodríguez-Barrueco R, et al. Autophagy orchestrates adaptive responses to targeted therapy in endometrial cancer. *Autophagy* 2017; 1–17.
- Mirantes C, Dosil MA, Eritja N, et al. Effects of the multikinase inhibitors Sorafenib and Regorafenib in PTEN deficient neoplasias. *Eur J Cancer* 2016; **63**: 74–87.
- Eritja N, Llobet D, Domingo M, et al. A novel three-dimensional culture system of polarized epithelial cells to study endometrial carcinogenesis. *Am J Pathol* 2010; **176**: 2722–2731.
- Eritja N, Mirantes C, Llobet D, et al. Long-term estradiol exposure is a direct mitogen for insulin/EGF-primed endometrial cells and drives PTEN loss-induced hyperplastic growth. *Am J Pathol* 2013; **183**: 277–287.
- Radu A, Neubauer V, Akagi T, et al. PTEN induces cell cycle arrest by decreasing the level and nuclear localization of cyclin D1. *Mol Cell Biol* 2003; **23**: 6139–6149.
- Paramio JM, Navarro M, Segrelles C, et al. PTEN tumour suppressor is linked to the cell cycle control through the retinoblastoma protein. *Oncogene* 1999; **18**: 7462–7468.
- Weng LP, Brown JL, Eng C. PTEN coordinates G(1) arrest by down-regulating cyclin D1 via its protein phosphatase activity and up-regulating p27 via its lipid phosphatase activity in a breast cancer model. *Hum Mol Genet* 2001; **10**: 599–604.
- Fantl V, Stamp G, Andrews A, et al. Mice lacking cyclin D1 are small and show defects in eye and mammary gland development. *Genes Dev* 1995; **9**: 2364–2372.
- Sicinski P, Donaher JL, Parker SB, et al. Cyclin D1 provides a link between development and oncogenesis in the retina and breast. *Cell* 1995; **82**: 621–630.
- Geng Y, Yu Q, Sicinska E, et al. Deletion of the p27Kip1 gene restores normal development in cyclin D1-deficient mice. *Proc Natl Acad Sci U S A* 2001; **98**: 194–199.
- Kozar K, Ciemerych MA, Rebel VI, et al. Mouse development and cell proliferation in the absence of D-cyclins. *Cell* 2004; **118**: 477–491.
- Fry DW, Harvey PJ, Keller PR, et al. Specific inhibition of cyclin-dependent kinase 4/6 by PD 0332991 and associated antitumor activity in human tumor xenografts. *Mol Cancer Ther* 2004; **3**: 1427–1438.
- Mirantes C, Dosil MA, Hills D, et al. Deletion of Pten in CD45-expressing cells leads to development of T-cell lymphoblastic lymphoma but not myeloid malignancies. *Blood* 2016; **127**: 1907–1911.
- Comstock CE, Augello MA, Goodwin JF, et al. Targeting cell cycle and hormone receptor pathways in cancer. *Oncogene* 2013; **32**: 5481–5491.

36. Bai F, Pei XH, Pandolfi PP, *et al.* p18 Ink4c and Pten constrain a positive regulatory loop between cell growth and cell cycle control. *Mol Cell Biol* 2006; **26**: 4564–4576.
37. Hydbring P, Malumbres M, Sicinski P. Non-canonical functions of cell cycle cyclins and cyclin-dependent kinases. *Nat Rev Mol Cell Biol* 2016; **17**: 280–292.
38. Asghar U, Witkiewicz AK, Turner NC, *et al.* The history and future of targeting cyclin-dependent kinases in cancer therapy. *Nat Rev Drug Discov* 2015; **14**: 130–146.
39. Sherr CJ, Beach D, Shapiro GI. Targeting CDK4 and CDK6: from discovery to therapy. *Cancer Discov* 2016; **6**: 353–367.
40. Clark AS, Karasic TB, DeMichele A, *et al.* Palbociclib (PD0332991) – a selective and potent cyclin-dependent kinase inhibitor: a review of pharmacodynamics and clinical development. *JAMA Oncol* 2016; **2**: 253–260.
41. Hidalgo M, Amant F, Biankin AV, *et al.* Patient-derived xenograft models: an emerging platform for translational cancer research. *Cancer Discov* 2014; **4**: 998–1013.
42. Malaney P, Nicosia SV, Davé V. One mouse, one patient paradigm: new avatars of personalized cancer therapy. *Cancer Lett* 2014; **344**: 1–12.
43. McClendon AK, Dean JL, Rivadeneira DB, *et al.* CDK4/6 inhibition antagonizes the cytotoxic response to anthracycline therapy. *Cell Cycle* 2012; **11**: 2747–2755.
44. Roberts PJ, Bisi JE, Strum JC, *et al.* Multiple roles of cyclin-dependent kinase 4/6 inhibitors in cancer therapy. *J Natl Cancer Inst* 2012; **104**: 476–487.
45. Dean JL, McClendon AK, Knudsen ES. Modification of the DNA damage response by therapeutic CDK4/6 inhibition. *J Biol Chem* 2012; **287**: 29075–29087.
46. Menu E, Garcia J, Huang X, *et al.* A novel therapeutic combination using PD 0332991 and bortezomib: study in the 5T33MM myeloma model. *Cancer Res* 2008; **68**: 5519–5523.
47. Baughn LB, Di Liberto M, Wu K, *et al.* A novel orally active small molecule potently induces G1 arrest in primary myeloma cells and prevents tumor growth by specific inhibition of cyclin-dependent kinase 4/6. *Cancer Res* 2006; **66**: 7661–7667.
48. Leonard JP, LaCasce AS, Smith MR, *et al.* Selective CDK4/6 inhibition with tumor responses by PD0332991 in patients with mantle cell lymphoma. *Blood* 2012; **119**: 4597–4607.
49. Meloche S, Pouyssegur J. The ERK1/2 mitogen-activated protein kinase pathway as a master regulator of the G1- to S-phase transition. *Oncogene* 2007; **26**: 3227–3239.

SUPPLEMENTARY MATERIAL ONLINE

Supplementary figure legends

Figure S1. Breeding scheme for the mice used in this study

Figure S2. *Pten* deletion causes an increase of Cyclin D1 and Ki-67 expression

Figure S3. Cyclin D1 is dispensable for *Pten* driven thyroid hyperplasias

Figure S4. Cyclin D1 is dispensable for *Pten* driven prostatic neoplasias

Figure S5. Cyclin D-CDK4/6 axis inhibition by palbociclib induces a decrease of cell proliferation *in vitro*

Figure S6. Palbociclib effects on *Pten* deficient thyroid hyperplasias

Figure S7. Palbociclib effects on *Pten* deficient prostate neoplasias

Figure S8. p-Rb IHC quantification and western blot analysis

Figure S9. Palbociclib treatment exhibits an anti-proliferative effect *in vitro* on human endometrial carcinoma cell lines

Table S1. Probes used for RT-qPCR

Table S2. Detailed specifications of the antibodies used for immunohistochemistry and western blotting